# Azimuthal Motion of Poleward Moving Auroral Forms

Jin Guo[1,2] ![ORCID], Boyi Wang[3] ![ORCID], San Lu[1,2] ![ORCID], Quanming Lu[1,2] ![ORCID], Yu Lin[4] ![ORCID], Xueyi Wang[4] ![ORCID], Rongsheng Wang[1,2] ![ORCID], Qinghe Zhang[5] ![ORCID], Zanyang Xing[5] ![ORCID], Yukitoshi Nishimura[6] ![ORCID], and Yen-Jung Wu[7]

[1]CAS Key Laboratory of Geospace Environment, School of Earth and Space Sciences, University of Science and Technology of China, Hefei, China, [2]CAS Center for Excellence in Comparative Planetology, Hefei, China, [3]Institute of Space Science and Applied Technology, Harbin Institute of Technology (Shenzhen), Shenzhen, China, [4]Physics Department, Auburn University, Auburn, AL, USA, [5]Shandong Provincial Key Laboratory of Optical Astronomy and Solar-Terrestrial Environment, Institute of Space Sciences, Shandong University, Weihai, China, [6]Department of Electrical and Computer Engineering and Center for Space Sciences, Boston University, Boston, MA, USA, [7]Space Sciences Laboratory, University of California Berkeley, Berkeley, CA, USA

**Abstract** Poleward moving auroral forms (PMAFs), the most common dayside auroral structure, images the process of energy and particle transport from the solar wind to the magnetosphere via magnetic reconnection. This form of aurora moves not only poleward, but also in the azimuthal (dawn-dusk) direction. However, the underlying mechanism responsible for the azimuthal motion of PMAFs are not thoroughly investigated. Here based on all-sky imager observations in the southern hemisphere, we statistically determine that the azimuthal motion of PMAFs is highly dependent on the dawn-dusk component of the interplanetary magnetic field (IMF $B_y$). Using three-dimensional (3-D) global hybrid simulations, we demonstrate that IMF $B_y$ controls the azimuthal motion of PMAFs through plasma flow derived from magnetic tension of magnetopause flux ropes. Our study, by focusing on the azimuthal motion of PMAFs, allows a better understanding of space weather, especially from a 3-D perspective.

**Plain Language Summary** Aurora is caused by energetic particles precipitating to the ionosphere along magnetic field lines. The aurora monitors the precipitation of energetic particles in the ionosphere that can give variable disturbances to space weather and impacts on telecommunications, electric power, satellite navigation, and other systems. Therefore, aurora is not only visually spectacular but also important for science and technology. Among many auroral phenomena, poleward moving auroral form (PMAF) is the most common dayside auroral structure, and it images the process of energy and particle transport from the solar wind to the magnetosphere and the ionosphere via magnetic reconnection. PMAFs have been reported to have significant azimuthal (dawn-dusk) propagations. However, the underlying mechanism responsible for the azimuthal motion of PMAFs are not thoroughly investigated. Thus, in this letter, by using all-sky-imager observations at the Automatic Geophysical Observatory P1 station, we show that the azimuthal motion of PMAFs is highly dependent on the dawn-dusk component of the interplanetary magnetic field (IMF $B_y$). Using 3-D global hybrid simulations, we demonstrate that IMF $B_y$ controls the azimuthal motion of PMAFs through plasma flow derived from magnetic tension.

## 1. Introduction

Aurora, a colorful and dynamic light display that illuminates Earth's polar regions, is caused by energetic particles precipitating to the ionosphere along magnetic field lines (Jones, 2012). The aurora is not only visually spectacular but also important in science because it monitors various dynamic processes during the interactions between the solar wind and the magnetosphere (Frey et al., 2003; Sandholt & Farrugia, 2003; Southwood, 1987). The interactions are dramatically intensified when the magnetic field in the solar wind, that is, interplanetary magnetic field (IMF), has a southward component and reconnects with the northward geomagnetic field at the dayside magnetopause (Dungey, 1961; Russell & Elphic, 1978). This reconnection process forms flux transfer events (FTEs) or flux ropes that correspond to the most common dayside auroral structure in the ionosphere, poleward moving auroral form (PMAF), which recurs every 5–15 min (Frey et al., 2019; Sandholt et al., 1986; Vorobjev et al., 1975; Wang, Nishimura, Zou, et al., 2016; Z. Xing et al., 2013).

The flux ropes are typically formed by magnetic reconnection at the low latitude magnetopause, then move poleward, and eventually merge into the cusp region (Guo et al., 2021a, 2021b; Hoilijoki et al., 2017; Omidi & Sibeck, 2007; Tan et al., 2012). Correspondingly, PMAFs typically brighten near the equatorward boundary of the dayside auroral oval, gradually move poleward, and eventually decay in the dayside polar cap in a few minutes (Frey et al., 2019; Sandholt et al., 1986; Z. Y. Xing et al., 2012). The mean lifetime of PMAFs is about 5 min (Fasel, 1995), and their poleward propagation speed is about 1 km/s (Oksavik et al., 2005; Wang, Nishimura, Lyons, et al., 2016). When PMAFs begin to decay in the polar cap, they can evolve into polar cap patches that can propagate across the polar cap and lead to nightside auroral activities (Lorentzen et al., 2010; Nishimura et al., 2014).

In addition to the poleward motion, PMAFs have also been observed to move in the azimuthal (dawn-dusk) direction in some early event studies (Sandholt et al., 2004; Sandholt & Farrugia, 2007a, 2007b; Wang, Nishimura, Lyons, et al., 2016; Zhang et al., 2010). Recently, Goertz et al. (2022) investigated the morphology of PMAFs in the northern hemisphere, including the azimuthal motion of PMAFs, which is consistent with the early event studies. However, the mechanism responsible for the azimuthal motion is worth further study. Here, we statistically determine that the azimuthal motion of PMAFs in the southern hemisphere also depends highly on the dawn-dusk component of the interplanetary magnetic field (hereinafter referred to as IMF $B_y$). We perform global-scale simulations to explain how IMF $B_y$ controls the azimuthal motion.

## 2. Methods

### 2.1. Instrument and Data Set

The optical imaging data were collected from the Automatic Geophysical Observatory (AGO) P1 station (83.86°S, 129.61°E in geographic coordinates; 80.14°S, 16.87°E in geomagnetic coordinates), from 2007 to 2011. We selected this station from the AGO network in Antarctica because it is centered around the poleward boundary of dayside auroral oval, which enables the observations of PMAFs from their appearance in the dayside auroral oval to their disappearance in the dayside polar cap. The all-sky imager (ASI) at P1 station records imager data every 1 min with two exposure times (Drury et al., 2003). The imaging data in this study are all recorded in long-exposure mode (8 s) in order to maximum the chance for detecting PMAFs. The ASI acquires imaging data in two different wavelengths (630.0 and 427.8 nm) and PMAFs are visible in both wavelengths. According to the altitude profile of the emissions, we mapped 630.0 and 427.8 nm emissions to the altitudes of 230 and 110 km, respectively (Dashkevich & Ivanov, 2019; Solomon et al., 1988).

With the 5-year data from P1 station, we automatically searched the optical imaging data from 9:30 to 21:30 UT during the winter season of the southern hemisphere. Because the magnetic local moon of P1 station is 15:30 UT and the field of view (FOV) of the ASI covers about 4 hr magnetic local time (MLT), the searching window of 9:30–21:30 UT can capture all the PMAFs occurring in the dayside region (i.e., from 8 to 16 MLT). Here, we have manually removed the snapshots with contaminations by sunlight, moonlight or clouds. PMAFs are identified in 630.0 nm emission as ~20 intensity units above background, associated with a poleward propagation of at least 0.1° in magnetic latitudinal direction. Here, the background is obtained by subtracting the average intensity over a 30-min window. Our automatic searching method obtained the propagation distances of PMAF in poleward and azimuthal directions, by tracing the brightest pixel in the processed snapshots within the field of view of the ASI at P1 station. In order to distinguish PMAFs from dayside airglow patches, we also require the intensification of 427.8 nm emission associated with PMAFs. We have manually checked the final data set and removed the wrong events that were incorrectly selected by our automatic searching code.

In order to investigate their azimuthal motions with IMF conditions, OMNI data set was utilized to calculate the background IMF of those PMAFs. Here, we consider an 8-min delay for dayside aurora responding to the IMF effects (Wang, Nishimura, Lyons, et al., 2016). With the data and the criteria presented above, we obtained 767 PMAFs occurring with southward IMF ($B_z < 0$; see Table S1 in Supporting Information S1).

### 2.2. Three-Dimensional Global Hybrid Simulation Model

In this study, we use a global hybrid simulation model to study the azimuthal motion of magnetopause flux ropes as PMAFs. In this model (Lin & Wang, 2005; Swift, 1996; Z. Guo et al., 2020), ions are treated as particles, and

electrons are treated as a massless fluid. In addition to the particle ions, a cold, incompressible ion fluid representing the plasmasphere is included in the inner magnetosphere. The magnetic field is advanced in time using Faraday's law, the electric field is calculated from the electron momentum equation, and the flow velocity of electrons is derived from Ampere's law.

A spherical coordinate system $(r, \theta, \varphi)$ is used, and the simulation domain includes a geocentric distance $3\,R_E \leq r \leq 27\,R_E$ (where $R_E$ is the Earth's radius), polar angle $0° < \theta < 180°$, and azimuth angle $10° < \varphi < 170°$. A total grid $N_r \times N_\varphi \times N_\theta = 400 \times 200 \times 200$ is used. To produce a higher resolution near the magnetopause, nonuniform grids are used in the $r$ direction with a smaller grid size of $\Delta r \approx 0.03\,R_E$ limited to $8\,R_E \leq r \leq 14\,R_E$. The Earth is located at $r = 0$. Outflow boundary conditions are utilized at the tailward boundary, and solar wind inflow boundary conditions are applied for the outer boundary at $r = 27\,R_E$. The inner boundary at $r = 3\,R_E$ is perfectly conducting. Initially, the Earth's dipole magnetic field is limited to $r \leq 10\,R_E$, and it interacts with the uniform solar wind placed in $r > 10\,R_E$. The geocentric solar-magnetospheric (GSM) coordinate is employed to describe the simulation results. The time step is $\Delta t = 0.05\Omega_i^{-1}$, where $\Omega_i$ is the unit ion gyrofrequency evaluated using the magnitude of magnetic field in the solar wind. About $8 \times 10^8$ particles are used in each simulation. A small current-dependent collision frequency is used to simulate the anomalous resistivity and trigger magnetic reconnection. The number density and magnetic field in the solar wind is $6\,cm^{-3}$ and $10\,nT$, respectively, corresponding to an Alfvén speed of $89\,km/s$ in the solar wind. The ion and electron plasma beta in the solar wind is $\beta_i = \beta_e = 0.5$. The solar wind is in the -$x$ direction, with a speed of $445\,km/s$, that is, the Alfven Mach number is $M_A = 5$. The scaled ion inertial length in the solar wind is $d_{i0} = 0.05\,R_E$.

## 3. Results

### 3.1. AGO P1 Observations

Using an automatic searching method (see Section 2), we obtained 767 PMAFs that occurred with a southward IMF from the 5 years all-sky-imager (ASI) data observed at the Automatic Geophysical Observatory (AGO) P1 station in the Antarctic (Mende et al., 1999), and the IMF condition is obtained from the OMNI data. We first select two representative PMAF events with IMF $B_y < 0$ and IMF $B_y > 0$, respectively, in order to show their azimuthal motions.

The first PMAF event occurred at about 15:39 UT on 3 June 2008, under a negative $B_y$-dominant IMF condition of about $(-0.46, -2.6, -1.2)$ nT in geocentric solar-magnetospheric (GSM) coordinates. As shown in Figures 1a–1d, the original 630 nm emission snapshots captured the high-latitude portion of dayside auroral oval and its poleward boundary at ~79°S in geomagnetic coordinates. The poleward boundary of auroral oval was steady at first (Figure 1a). At ~15:39 UT, there was bright aurora arc with its brightest part at about 12.2 hr magnetic local time (MLT) in the post-noon sector (highlighted by the dashed magenta circle in Figures 1b and 1f). Here, one MLT grid on the maps is 1 hour. In order to show this transient structure better, the original snapshots were subtracted by the average of the intensity over 30 min, and the results are shown in Figures 1e–1h. This bright structure was associated with an intensification in 427.8 nm emission, as shown in Figures 1j–1l. It indicates that this structure came with energetic electron precipitation, which was an auroral structure but not an airglow enhancement. The further poleward motion of this auroral structure (shown in Figures 1f–1h) determines that it is a PMAF. It is noted that the PMAF moved azimuthally to about 11.74 hr MLT in the pre-noon sector during its poleward propagation toward the dayside polar cap.

The second PMAF event occurred at about 15:43 UT on 11 May 2010, under a positive $B_y$-dominant IMF condition of about $(-2.6, 5.8, -2.1)$ nT in GSM coordinates. Figures 1m–1p show that, similar to the first event, the original 630 nm emission snapshots captured the dayside auroral oval and the dayside polar cap. The poleward auroral oval boundary was at ~80°S in geomagnetic coordinates. By subtracting a 30-min averaged background, a transient structure emerged and brightened near the dayside auroral oval boundary, as shown in Figure 1n. This bright structure came with energetic particle precipitation, as indicated by the intensification of the 427.8 nm emission along with the structure. The bright structure continued to move poleward and duskward. Therefore, this bright structure can be identified as a PMAF. This PMAF moved azimuthally from about 11.5 to 12.5 hr MLT, in the direction opposite to that in the first event.
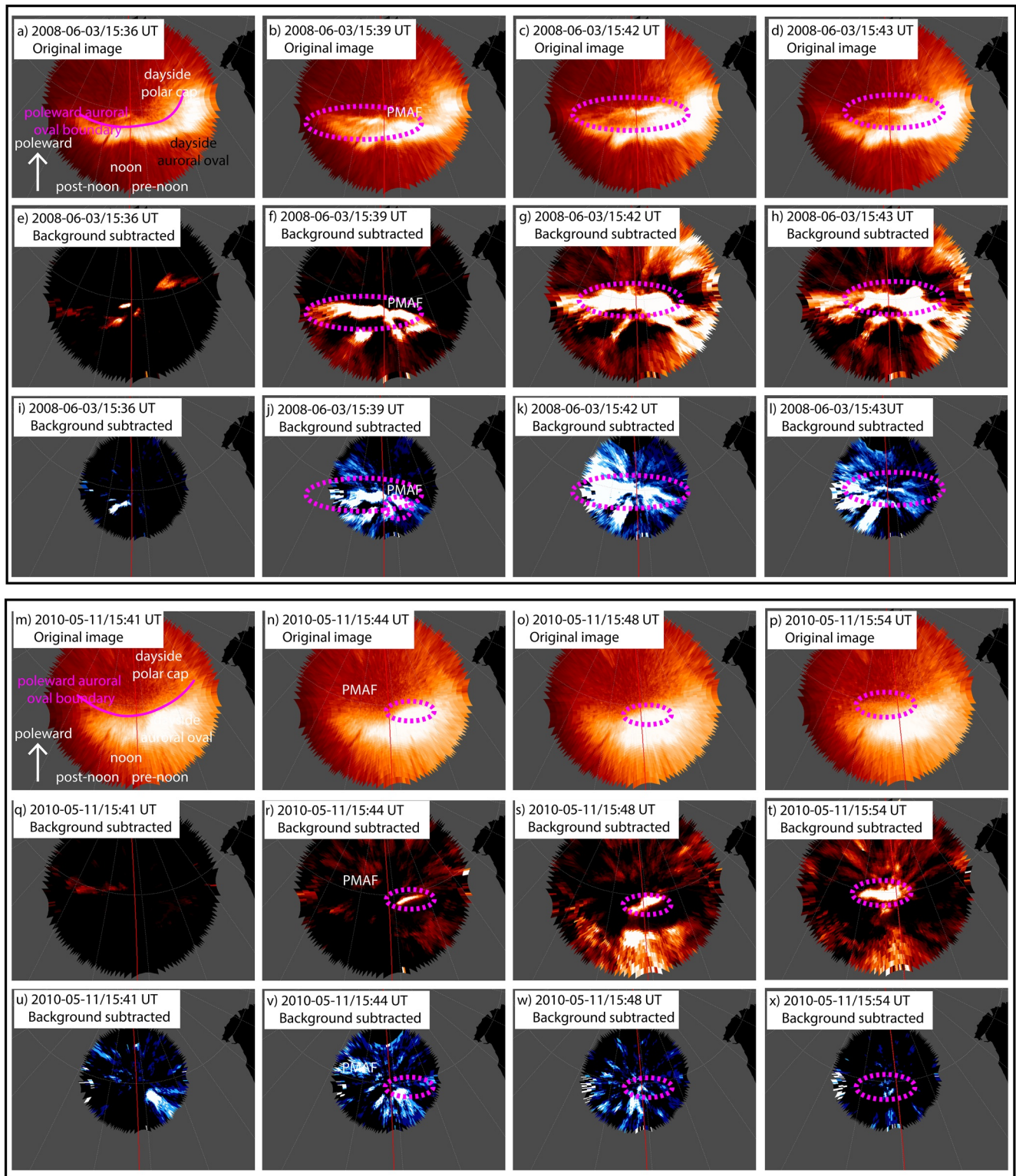
**Figure 1.** All-sky imager observations of two poleward moving auroral form (PMAF) events at Automatic Geophysical Observatory P1 station. The first three rows show Event 1, dawnward motion of a PMAF with a negative interplanetary magnetic field (IMF $B_y$) on 3 June 2008 (a–d) original snapshots of 630.0 nm emission at 15:36, 15:39, 15:42 and 15:43 UT, respectively (e–h) the background-subtracted snapshots of 630.0 nm emission at the same time of the snapshots in (a–d) (i–l) the background-subtracted snapshots of 427.8 nm emission at the same time of the snapshots in (a–d), respectively. The last three rows show Event 2, duskward motion of another PMAF with a positive IMF $B_y$ on 11 May 2010 (m–x) same formats as (a–l), respectively, except that those snapshots were taken at 15:41, 15:44, 15:48 and 15:54 UT on 11 May 2010.
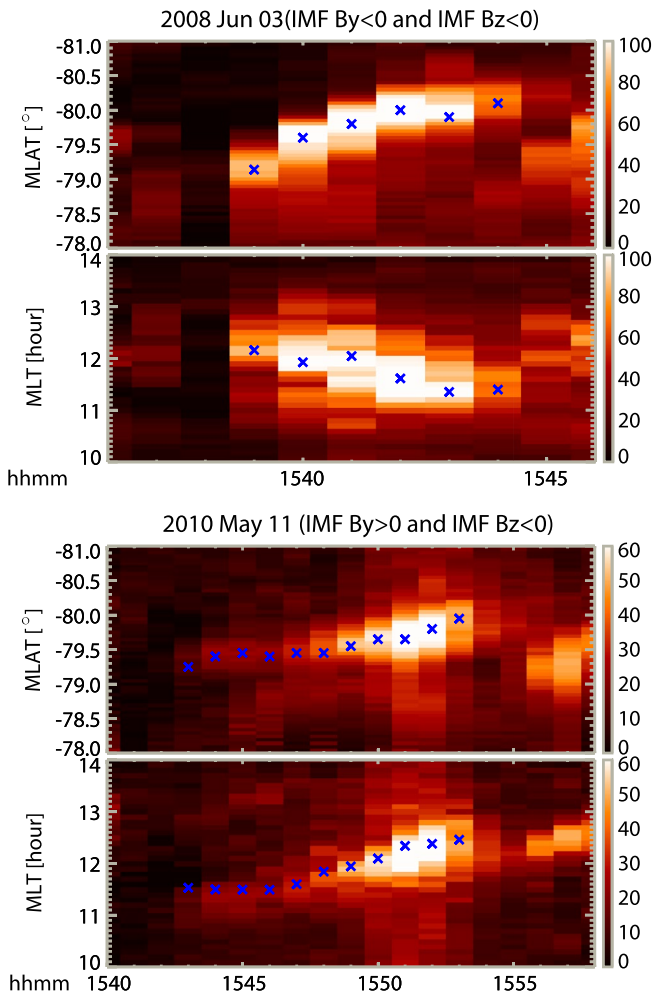
**Figure 2.** Keograms for the two events in Figures 1a and 1b Event 1, north-south keograms and dawn-dusk keograms (in the unit of magnetic local time), respectively, of 630.0 nm emissions observed at Automatic Geophysical Observatory P1 station on 3 June 2008. (c and d) Event 2, same format as (a and b), on 11 May 2010.

Figure 2 shows the keograms for the two representative PMAF events described above. It is clear that our automatic searching method well-identifies the PMAF positions (the blue crosses in Figure 2). The north-south keograms in Figures 2a and 2c show that those two structures moved poleward by 0.9° and 0.7° magnetic latitude (MLAT), respectively. The dawn-dusk keograms in Figures 2a and 2c show the azimuthal motion of the two PMAFs. The first event occurred under IMF $B_y < 0$, with a lifetime of ~5 min and a dawnward propagation of ~0.75 hr MLT. The second event occurred under IMF $B_y > 0$, with a lifetime of ~10 min and a duskward propagation of ~0.93 hr MLT.

The two events above support the idea that the azimuthal motion of PMAFs depends on the IMF $B_y$. To investigate the generalization of such dependence, a statistical analysis is performed on the basis of the 767 PMAF events under the southward IMF condition. Figures 3a and 3b show the azimuthal motion of PMAFs as a function of the distance (ΔMLT) that the PMAFs propagate during their lifetime. As shown in Figure 3a, for 403 PMAF events with IMF $B_y < 0$ and IMF $B_z < 0$, about 74% (297 events) of PMAFs propagated dawnward by a maximum of 1.9 hr MLT and a median of 0.23 hr MLT. As shown in Figure 3b, for 364 PMAF events with IMF $B_y > 0$ and IMF $B_z < 0$, 72% (262 events) of PMAFs propagated duskward by a maximum of 2.1 hr MLT and a median of 0.17 hr MLT. Figure 3c shows the relationship between ΔMLT of PMAF events and IMF $B_y$. The azimuthal motion of PMAFs strongly depends on the corresponding IMF $B_y$. When the magnitude of IMF $B_y$ becomes larger, PMAFs tend to move dawnward or duskward further away from noon. This dependence can be linearly fitted well. The slope indicates that when the $B_y$ component of the IMF increases (decreases) by 1 nT, the PMAF will roughly move duskward (dawnward) for about 0.36 hr MLT.

We also investigate the role of IMF $B_y$ in the average speed of the azimuthal motions of these PMAFs. Figures 3d and 1e show that the median values of the PMAF events with IMF $B_y < 0$ and IMF $B_y > 0$ are about −0.059 hr MLT per minute and 0.046 hr MLT per minute. The dependence of the average azimuthal speed of these PMAFs on IMF $B_y$ is linearly fitted well as shown in Figure 3f. The slope indicates that when the $B_y$ component of the IMF increases (decreases) by 1 nT, the average azimuthal speed of PMAF will roughly increase (decrease) for about 0.072 hr MLT per minute in the duskward direction.

In the next section, we will investigate the strong dependence of PMAFs' azimuthal motions on IMF $B_y$ by comparing these with our global hybrid simulation results.

### 3.2. Three-Dimensional Global Hybrid Simulations

PMAFs are known as the ionospheric signature of FTEs or magnetopause flux ropes (Fasel et al., 1994; Lee & Fasel, 1994; Ma et al., 1995; Omidi & Sibeck, 2007). To explain the observed azimuthal motion of PMAFs, we perform three-dimensional (3-D) global hybrid simulations of magnetopause flux ropes with an IMF of (0, −7.07, −7.07) nT in the GSM coordinates.

In Figure 4a, the flux ropes "1–7" with parallel temperature enhancements are formed by multiple X-line reconnection in the noon-midnight meridian plane (Guo et al., 2021b, 2021c; Lee & Fu, 1985; Lee et al., 1993; Tan et al., 2011). These flux ropes are formed at low latitudes and then move to higher latitudes. For example, in Figure 4b, flux rope "2" moves poleward from −12° ($t = 169$ s) to −45° (at $t = 321$ s) MLAT. Eventually, these flux ropes merge into the cusp region, leading to an enhancement in ion temperature therein (J. Guo et al., 2021a; Omidi & Sibeck, 2007). By mapping the flux ropes to the ionosphere, the corresponding PMAFs form at the
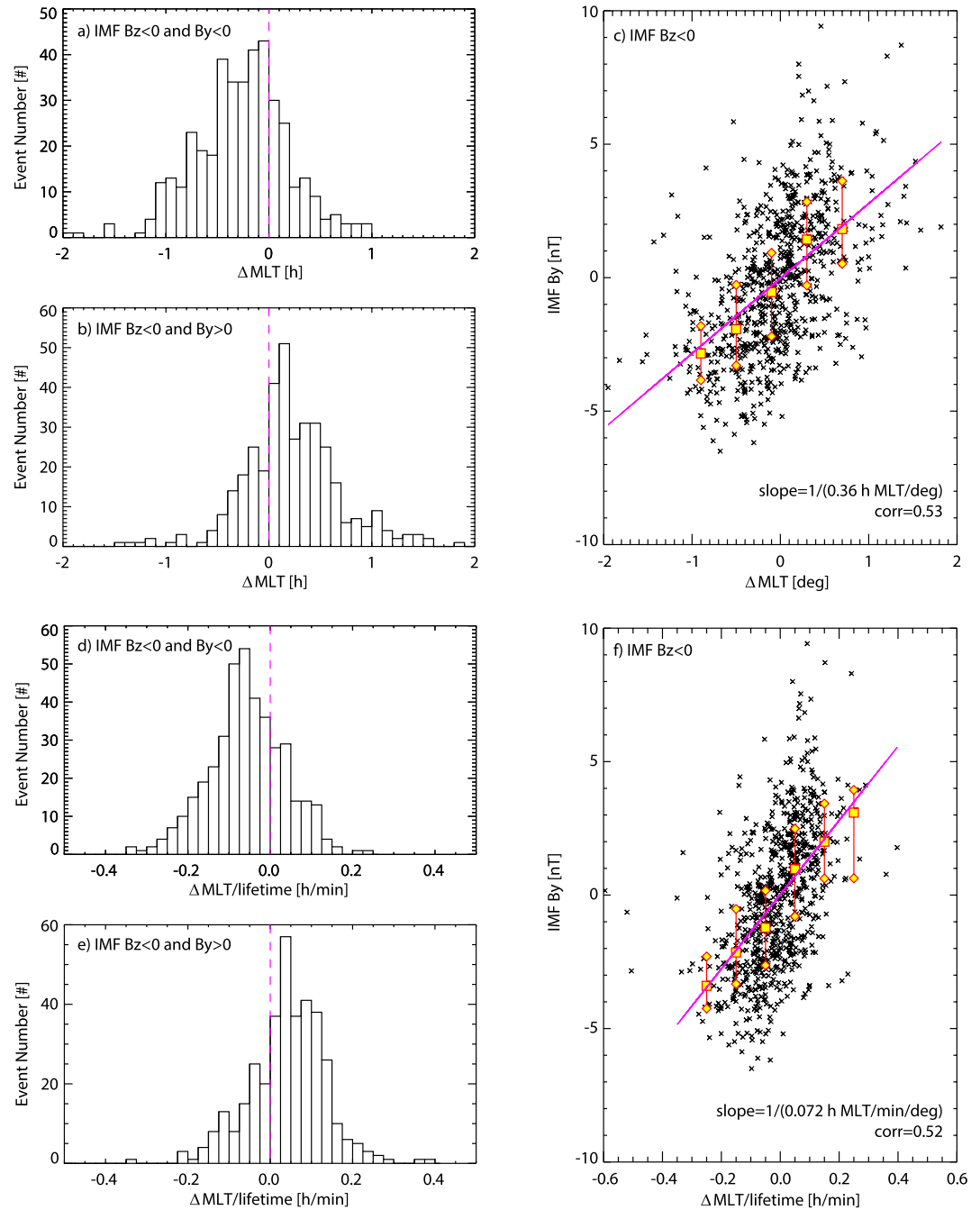
**Figure 3.** Statistical analysis of the azimuthal motion of poleward moving auroral form (PMAF) events and its relationship with interplanetary magnetic field (IMF $B_y$). (a) and (b) Number of PMAF events as a function of the magnetic local time (MLT) changes ($\Delta$MLT) due to azimuthal motions, under (a) IMF $B_y < 0$ and IMF $B_z < 0$ and (b) IMF $B_y > 0$ and IMF $B_z < 0$, respectively. (c) Relationship between $\Delta$MLT of PMAF events and IMF $B_y$. The squares and diamonds (error bars) indicate the medians and upper/lower quartiles every 0.4 hr MLT. (d and e) are in the same format of (a and b) except that the event numbers are shown as a function of $\Delta$MLT/lifetime. (f) Relationship between $\Delta$MLT/lifetime of PMAF events and IMF $B_y$. The squares and diamonds (error bars) indicate the medians and upper/lower quartiles every 0.1 hr MLT/min.

equatorward boundary of the dayside auroral oval, move poleward, and eventually vanish at the polar cap. Figure 4b shows the azimuthal motion of a representative flux rope (flux rope "1" in Figure 4a) in the southern hemisphere. The flux rope is characterized by a helical field line structure and an enhancement in the ion parallel temperature, based on which we determine the position of the flux rope. As shown in Figure 4b, at $t = 169$ s, the center of
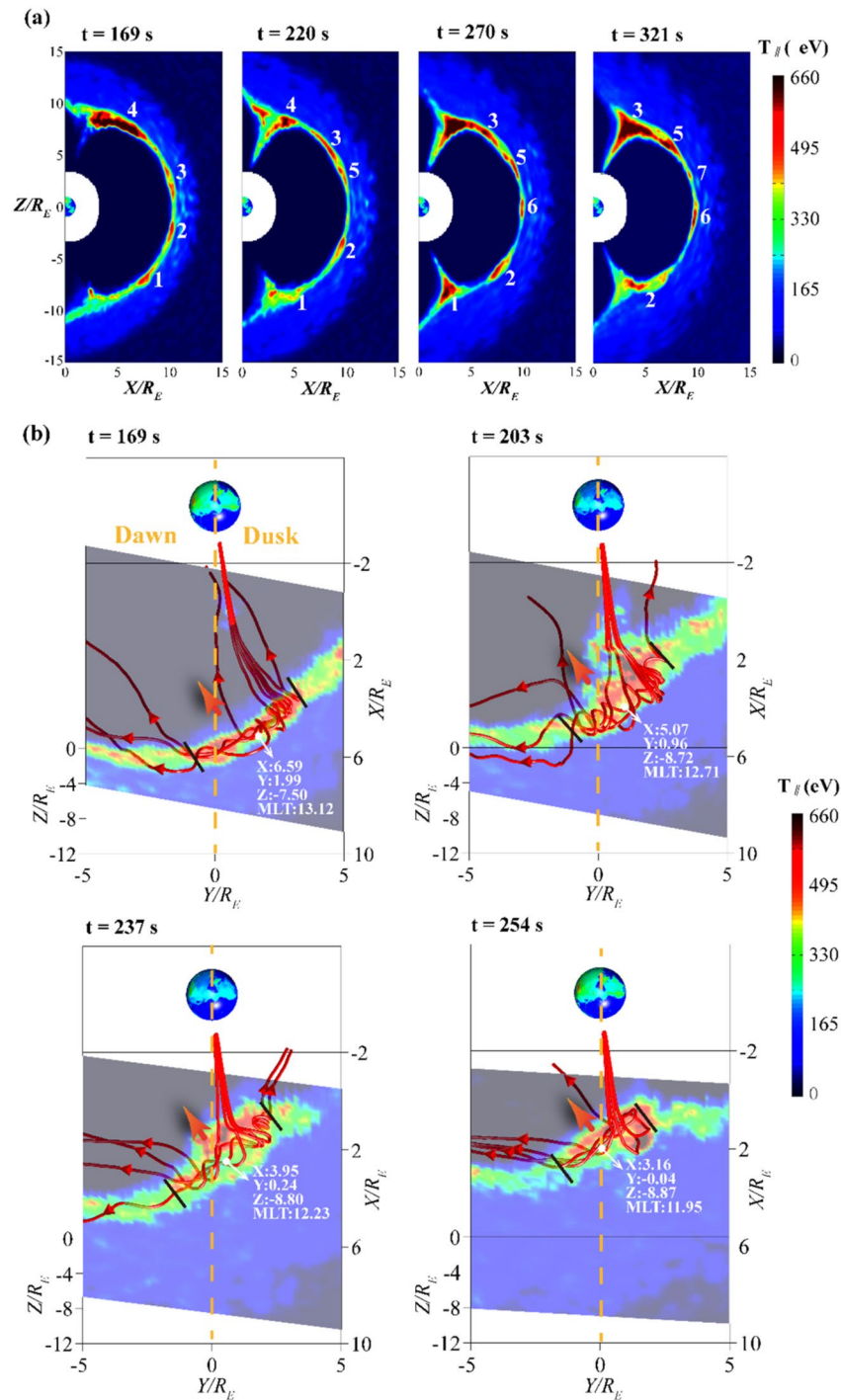
**Figure 4.** (a) Ion parallel temperature $T_\parallel$ (eV) in the noon-midnight meridian plane at $t$ = 169, 220, 270, and 321 s. The white numbers represent the flux ropes. (b) Ion parallel temperature $T_\parallel$ (eV) at $t$ = 169, 203, 237, and 254 s. The slice of parallel temperature is tilted to keep it along the axial direction of the flux rope. The flux rope represented by red field lines is flux rope "1" in (a). The plasma around the flux rope has a high parallel temperature. Here, its boundary is determined by the temperature enhancement ($T_\parallel > 400$ eV) and the helical field lines of this flux rope. Then, we can identify the center of the flux rope by its boundary (black lines) and calculate its corresponding magnetic local time (MLT). The central coordinate and central MLT are shown by white letters and dots. The dashed lines represent the noon-midnight meridian plane, and the orange arrows represents the motion of the flux rope.

the flux rope is at 13.12 hr MLT ($x = 6.59\ R_E$, $y = 1.99\ R_E$, $z = −7.50\ R_E$); at $t = 254$ s, the center of the flux rope moves to 11.95 hr MLT ($x = 3.16\ R_E$, $y = −0.04\ R_E$, $z = −8.87\ R_E$). This means that the flux rope moves dawnward for about 1.17 hr MLT and moves toward the south pole for about 2.2° MLAT in 85 s. Therefore, in the southern hemisphere and with a negative IMF $B_y$, PMAF, as the ionospheric signature of the flux rope, should also move dawnward, which is consistent with our statistical result from observations (Figures 3a and 3c). The lifetime (∼3 min) of the flux rope is consistent with that of the PMAF (Figure 2b), but the azimuthal velocity of the flux rope is faster than that of PMAF (Figure 2b), which may be due to the faster magnetopause reconnection and outflows caused by the strong IMF in the solar wind. We also perform a simulation with a positive IMF $B_y$, and in the case, the representative flux rope in the southern hemisphere moves duskward for about 1.58 hr MLT
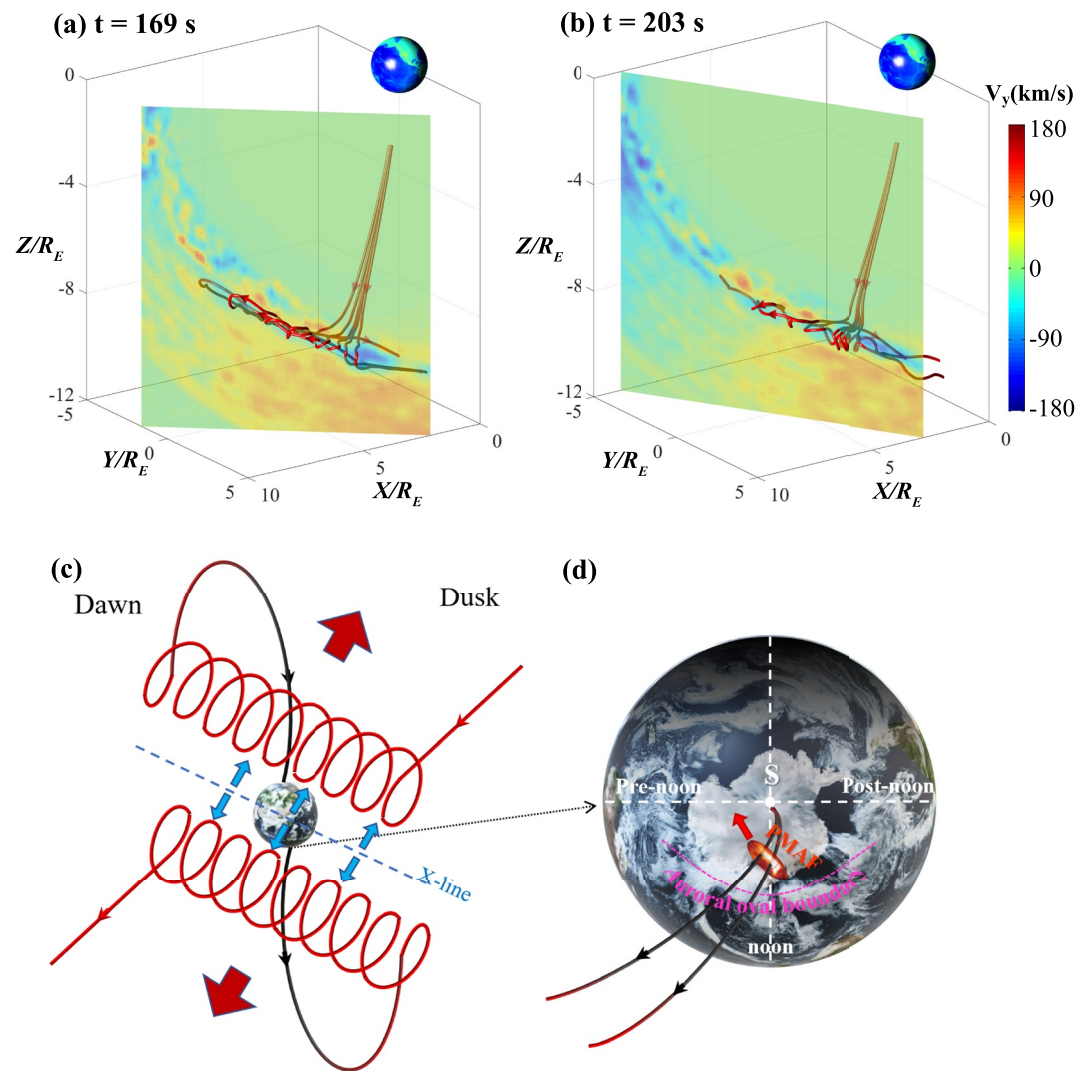


**Figure 5.** (a and b) Ion velocity in the y-direction $V_y$ (km/s) at $t = 169$ and 203 s. The flux rope characterized by red magnetic field lines is flux rope "1" in Figure 4. The slice of $V_y$ is tilted to keep it along the axial direction of the flux rope. (c) Schematic of the azimuthal motion of poleward moving auroral forms (PMAFs) when the interplanetary magnetic field (IMF $B_y$) is negative. The helical curves with arrows are the magnetic field lines of flux ropes. The blue dashed line represents the tilted X-line near the equator. Blue arrows on either side of the X-line represent the reconnection outflows that push the flux ropes to the south (north) pole and the dawnside (duskside). The red arrows next to the flux ropes represent the magnetic tensions which pull the flux ropes to the south (north) pole and the dawnside (duskside). (d) A zoom-in view of the Earth's southern hemisphere when the PMAFs occur with a negative IMF $B_y$. The black curves with arrows are the magnetic field lines connected from the Earth to the flux ropes. By mapping the flux ropes to the ionosphere, the corresponding PMAFs occur at the equatorward boundary of the dayside auroral oval (donated by magenta dashed curves). The motion of the flux ropes in the southern hemisphere corresponds to the dawnward and poleward motion of PMAFs.

(see Figure S1 in Supporting Information S1). The corresponding PMAF in the southern hemisphere should also moves duskward, consistent with our statistical result from observations (Figures 3b and 3c).

Figures 5a and 5b show the ion velocity in the dawn-dusk direction, $V_y$. The flux rope (the flux rope "1" in Figure 4) is surrounded by the duskward magnetosheath flow with $V_y > 0$, whereas the ion flow is dawnward ($V_y < 0$) in the flux rope, opposite to the surrounded magnetosheath flow. This shows that the flux rope moves dawnward because of the dawnward flow in the flux rope. Based on the above simulation results, Figures 5c and 5d summarize how the IMF $B_y$ controls the azimuthal motion of PMAFs. With $B_y < 0$, the X-line of magnetopause reconnection tilts, unparallel to the equatorial plane (Guo et al., 2021a, 2021b, 2021c). Thus, the reconnection outflows (blue arrows in Figure 5c) from the tilted X-line are dawnward and poleward in the southern hemisphere, and they push the magnetopause flux ropes dawnward and poleward. The reconnection outflows are derived from the magnetic tension (red arrows in Figure 5c, which is dawnward and poleward in the southern hemisphere) of the reconnected semi-open field lines (connected from the magnetosphere to IMF). As a result, the corresponding PMAF also moves poleward and dawnward (Figure 5d).

## 4. Conclusions and Discussion

Based on the statistical analysis of 767 PMAFs under southward IMF condition that were observed at the AGO P1 station in the southern hemisphere, we show that the azimuthal motion of PMAFs is highly dependent on the polarity of the IMF $B_y$. About 74% PMAFs with IMF $B_y < 0$ propagated dawnward with a median of 0.23 hr MLT and a maximum of 1.9 hr MLT, and 72% PMAFs with IMF $B_y > 0$ propagated duskward with a median of 0.17 hr MLT and a maximum of 2.1 hr MLT. Because PMAFs are known as the ionospheric signatures of magnetopause flux ropes (or FTEs), by performing 3-D global hybrid simulations, we show that the magnetopause flux ropes in the southern hemisphere typically move dawnward for ~1.17 hr MLT and duskward for ~1.58 hr MLT with IMF $B_y < 0$ and $B_y > 0$, respectively, in excellent agreement with the observations of PMAFs. We demonstrate that the azimuthal motion of PMAFs is originated from that of magnetopause flux ropes controlled by the IMF $B_y$ through plasma flow derived from magnetic tension.

Flux ropes are formed by the dayside patchy magnetic reconnection, which manifest as FTEs in spacecraft observations (Hasegawa et al., 2010; Lee & Fu, 1985). These flux ropes or FTEs can transfer energy and particles from the solar wind to the Earth's magnetosphere. They can further affect the coupled magnetosphere and ionosphere system by electron precipitations and field-aligned currents, as indicated by the occurrence of PMAFs. Furthermore, the observation of PMAFs and simulation of flux ropes both indicates that such energy and particle transportation across the magnetopause can extend toward dawn or dusk under IMF $B_y$-dominant conditions, and the geo-effects will cover larger areas with lager IMF $B_y$. On the other hand, the optical imaging observation of PMAFs can continuously records and monitors the evolution and azimuthal motions of flux ropes in a 2-D perspective, and our hybrid simulation can forecast such space weather events in a 3-D perspective.

## Data Availability Statement

The optical imaging data at AGO P1 station can be accessed online (http://sprg.ssl.berkeley.edu/atmos/ago_data.html). The authors gratefully acknowledge the data resources from the "National Space Science Data Center, National Science & Technology Infrastructure of China (http://www.nssdc.ac.cn)." The simulation data and the complete AGO P1 event list (i.e., Table S1 in Supporting Information S1) can be downloaded from https://dx.doi.org/10.12176/01.99.02442.

## References

Dashkevich, Z. V., & Ivanov, V. E. (2019). Estimated nitric oxide density in auroras from ground-based photometric data. *Solar-Terrestrial Physics*, *5*(1), 77–81. https://doi.org/10.12737/stp-51201908

Drury, E. E., Mende, S. B., Frey, H. U., & Doolittle, J. H. (2003). Southern Hemisphere poleward moving auroral forms. *Journal of Geophysical Research*, *108*(A3), 1114. https://doi.org/10.1029/2001JA007536

Dungey, J. W. (1961). Interplanetary magnetic field and the auroral zones. *Physical Review Letters*, *6*(2), 47–48. https://doi.org/10.1103/PhysRevLett.6.47

Fasel, G. J. (1995). Dayside poleward moving auroral forms: A statistical study. *Journal of Geophysical Research*, *100*(A7), 11891–11905. https://doi.org/10.1029/95JA00854

Fasel, G. J., Minow, J. I., Smith, R. W., Deehr, C. S., & Lee, L. C. (1994). *Multiple brightenings of poleward-moving dayside auroral forms* (Vol. 81, pp. 201–211). American Geophysical Union Geophysical Monograph Series. https://doi.org/10.1029/GM081p0201

Frey, H. U., Han, D., Kataoka, R., Lessard, M. R., Milan, S. E., Nishimura, Y., et al. (2019). Dayside aurora. *Space Science Reviews*, *215*(8), 51. https://doi.org/10.1007/s11214-019-0617-7

Frey, H. U., Phan, T. D., Fuselier, S. A., & Mende, S. B. (2003). Continuous magnetic reconnection at Earth's magnetopause. *Nature*, *426*(6966), 533–537. https://doi.org/10.1038/nature02084

Goertz, A. O., Partamies, N., Whiter, D., & Baddeley, L. (2022). The morphology of poleward moving auroral forms. EGUsphere. https://doi.org/10.5194/egusphere-2022-296

Guo, J., Lu, S., Lu, Q., Lin, Y., Wang, X., Huang, K., et al. (2021a). Re-reconnection processes of magnetopause flux ropes: Three-dimensional global hybrid simulations. *Journal of Geophysical Research: Space Physics*, *126*(6), e2021JA029388. https://doi.org/10.1029/2021JA029388

Guo, J., Lu, S., Lu, Q., Lin, Y., Wang, X., Huang, K., et al. (2021b). Structure and coalescence of magnetopause flux ropes and their dependence on IMF clock angle: Three-dimensional global hybrid simulations. *Journal of Geophysical Research: Space Physics*, *126*(2), e2020JA028670. https://doi.org/10.1029/2020JA028670

Guo, J., Lu, S., Lu, Q., Lin, Y., Wang, X., Zhang, Q., et al. (2021c). Three-dimensional global hybrid simulations of high latitude magnetopause reconnection and flux ropes during the northward IMF. *Geophysical Research Letters*, *48*(21), e2021GL095003. https://doi.org/10.1029/2021GL095003

Guo, Z., Lin, Y., Wang, X., Vines, S. K., Lee, S. H., & Chen, Y. (2020). Magnetopause reconnection as influenced by the dipole tilt under southward IMF conditions: Hybrid simulation and MMS observation. *Journal of Geophysical Research: Space Physics*, *125*(9). https://doi.org/10.1029/2020JA027795

Hasegawa, H., Wang, J., Dunlop, M. W., Pu, Z. Y., Zhang, Q.-H., Lavraud, B., et al. (2010). Evidence for a flux transfer event generated by multiple X-line reconnection at the magnetopause. *Geophysical Research Letters*, *37*(16), L16101. https://doi.org/10.1029/2010GL044219

Hoilijoki, S., Ganse, U., Pfau-Kempf, Y., Cassak, P. A., Walsh, B. M., Hietala, H., et al. (2017). Reconnection rates and X line motion at the magnetopause: Global 2D-3V hybrid-Vlasov simulation results. *Journal of Geophysical Research: Space Physics*, *122*(3), 2877–2888. https://doi.org/10.1002/2016JA023709

Jones, A. V. (2012). *Aurora* (Vol. 9). Springer Science & Business Media.

Lee, L. C., & Fasel, G. J. (1994). Patchy multiple X-line reconnection and poleward-moving auroral forms. In *Physical signatures of magnetospheric boundary layer processes* (pp. 291–306). https://doi.org/10.1007/978-94-011-1052-5_20

Lee, L. C., & Fu, Z. F. (1985). A theory of magnetic flux transfer at the Earth's magnetopause. *Geophysical Research Letters*, *12*(2), 105–108. https://doi.org/10.1029/GL012i002p00105

Lee, L. C., Ma, Z. W., Fu, Z. F., & Otto, A. (1993). Topology of magnetic flux ropes and formation of fossil flux transfer events and boundary layer plasmas. *Journal of Geophysical Research*, *98*(A3), 3943–3951. https://doi.org/10.1029/92JA02203

Lin, Y., & Wang, X. Y. (2005). Three-dimensional global hybrid simulation of dayside dynamics associated with the quasi-parallel bow shock. *Journal of Geophysical Research*, *110*(A12), A12216. https://doi.org/10.1029/2005JA011243

Lorentzen, D. A., Moen, J., Oksavik, K., Sigernes, F., Saito, Y., & Johnsen, M. G. (2010). In situ measurement of a newly created polar cap patch. *Journal of Geophysical Research*, *115*(A12). https://doi.org/10.1029/2010JA015710

Ma, Z. W., Lee, L. C., & Otto, A. (1995). Generation of field-aligned currents and Alfvén waves by 3D magnetic reconnection. *Geophysical Research Letters*, *22*(13), 1737–1740. https://doi.org/10.1029/95GL01430

Mende, S. B., Frey, H. U., Geller, S. P., & Doolittle, J. H. (1999). Multistation observations of auroras: Polar cap substorms. *Journal of Geophysical Research*, *104*(A2), 2333–2342. https://doi.org/10.1029/1998JA900084

Nishimura, Y., Lyons, L. R., Zou, Y., Oksavik, K., Moen, J. I., Clausen, L. B., et al. (2014). Day-night coupling by a localized flow channel visualized by polar cap patch propagation. *Geophysical Research Letters*, *41*(11), 3701–3709. https://doi.org/10.1002/2014GL060301

Oksavik, K., Moen, J., Carlson, H. C., Greenwald, R. A., Milan, S. E., Lester, M., et al. (2005). Multi-instrument mapping of the small-scale flow dynamics related to a cusp auroral transient. *Annales Geophysicae*, *23*(7), 2657–2670. https://doi.org/10.5194/angeo-23-2657-2005

Omidi, N., & Sibeck, D. G. (2007). Flux transfer events in the cusp. *Geophysical Research Letters*, *34*(4), L04106. https://doi.org/10.1029/2006GL028698

Russell, C. T., & Elphic, R. C. (1978). Initial ISEE magnetometer results: Magnetopause observations. *Space Science Reviews*, *22*(6), 681–715. https://doi.org/10.1007/BF00212619

Sandholt, P. E., Deehr, C. S., Egeland, A., Lybekk, B., Viereck, R., & Romick, G. J. (1986). Signatures in the dayside aurora of plasma transfer from the magnetosheath. *Journal of Geophysical Research*, *91*(A9), 10063–10079. https://doi.org/10.1029/JA091iA09p10063

Sandholt, P. E., & Farrugia, C. J. (2003). Does the aurora provide evidence for the occurrence of antiparallel magnetopause reconnection? *Journal of Geophysical Research*, *108*(A12), 1466. https://doi.org/10.1029/2003JA010066

Sandholt, P. E., & Farrugia, C. J. (2007a). Poleward moving auroral forms (PMAFs) revisited: Responses of aurorae, plasma convection and Birkeland currents in the pre- and postnoon sectors under positive and negative IMF $B_y$ conditions. *Annales Geophysicae*, *25*(7), 1629–1652. https://doi.org/10.5194/angeo-25-1629-2007

Sandholt, P. E., & Farrugia, C. J. (2007b). Role of poleward moving auroral forms in the dawn-dusk auroral precipitation asymmetries induced by IMF by. *Journal of Geophysical Research*, *112*(A4). https://doi.org/10.1029/2006JA011952

Sandholt, P. E., Farrugia, C. J., & Denig, W. F. (2004). Dayside aurora and the role of IMF| B y|/| B z|: Detailed morphology and response to magnetopause reconnection. *Annales Geophysicae*, *22*, 613–628. https://doi.org/10.5194/angeo-22-613-2004

Solomon, S. C., Hays, P. B., & Abreu, V. J. (1988). The auroral 6300 Å emission: Observations and modeling. *Journal of Geophysical Research*, *93*(A9), 9867–9882. https://doi.org/10.1029/JA093iA09p09867

Southwood, D. J. (1987). The ionospheric signature of flux transfer events. *Journal of Geophysical Research*, *92*(A4), 3207–3213. https://doi.org/10.1029/JA092iA04p03207

Swift, D. W. (1996). Use of a hybrid code for global-scale plasma simulation. *Journal of Computational Physics*, *126*(1), 109–121. https://doi.org/10.1006/jcph.1996.0124

Tan, B., Lin, Y., Perez, J. D., & Wang, X. Y. (2011). Global-scale hybrid simulation of dayside magnetic reconnection under southward IMF: Structure and evolution of reconnection. *Journal of Geophysical Research*, *116*(A2), A02206. https://doi.org/10.1029/2010JA015580

Tan, B., Lin, Y., Perez, J. D., & Wang, X. Y. (2012). Global-scale hybrid simulation of cusp precipitating ions associated with magnetopause reconnection under southward IMF. *Journal of Geophysical Research*, *117*(A3). https://doi.org/10.1029/2011JA016871

Vorobjev, V. G., Gustafsson, G., Starkov, G. V., Feldstein, Y. I., & Shevnina, N. F. (1975). Dynamics of day and night aurora during substorms. *Planetary and Space Science*, *23*(2), 269–278. https://doi.org/10.1016/0032-0633(75)90132-4

Wang, B., Nishimura, Y., Lyons, L. R., Zou, Y., Carlson, H. C., Frey, H. U., & Mende, S. B. (2016). Analysis of close conjunctions between dayside polar cap airglow patches and flow channels by all-sky imager and DMSP. *Earth Planets and Space*, *68*(1), 1–12. https://doi.org/10.1186/s40623-016-0524-z

Wang, B., Nishimura, Y., Zou, Y., Lyons, L. R., Angelopoulos, V., Frey, H., & Mende, S. (2016). Investigation of triggering of poleward moving auroral forms using satellite-imager coordinated observations. *Journal of Geophysical Research: Space Physics*, *121*(11), 10–929. https://doi.org/10.1002/2016JA023128

Xing, Z., Yang, H., Han, D., Wu, Z., Liu, J., Hu, Z., et al. (2013). Dayside poleward moving auroral forms and ionospheric convection under stable interplanetary magnetic field (IMF) conditions. *Science China Technological Sciences*, *56*(4), 910–916. https://doi.org/10.1007/s11431-013-5164-y

Xing, Z. Y., Yang, H. G., Han, D. S., Wu, Z. S., Hu, Z. J., Zhang, Q. H., et al. (2012). Poleward moving auroral forms (PMAFs) observed at the yellow river station: A statistical study of its dependence on the solar wind conditions. *Journal of Atmospheric and Solar-Terrestrial Physics*, *86*, 25–33. https://doi.org/10.1016/j.jastp.2012.06.004

Zhang, Q. H., Dunlop, M. W., Lockwood, M., Liu, R. Y., Hu, H. Q., Yang, H. G., et al. (2010). Simultaneous observations of reconnection pulses at Cluster and their effects on the cusp aurora observed at the Chinese Yellow River Station. *Journal of Geophysical Research*, *115*(A10). https://doi.org/10.1029/2010JA015526